We are IntechOpen,
the world's leading publisher of Open Access books
Built by scientists, for scientists

4,800
Open access books available

122,000
International authors and editors

135M
Downloads

Our authors are among the

154
Countries delivered to

TOP 1%
most cited scientists

12.2%
Contributors from top 500 universities

CLARIVATE ANALYTICS
BOOK CITATION INDEX
INDEXED

WEB OF SCIENCE™

Selection of our books indexed in the Book Citation Index
in Web of Science™ Core Collection (BKCI)

Interested in publishing with us?
Contact book.department@intechopen.com

Numbers displayed above are based on latest data collected.
For more information visit www.intechopen.com

Effects of Grain Refining on Columnar-to-Equiaxed Transition in Aluminum Alloys

Hicham Tahiri, Serageldin S. Mohamed,
Herbert W. Doty, Salvador Valtierra and
Fawzy H. Samuel

Additional information is available at the end of the chapter

Abstract

The effects of grain refining in ultra-pure aluminum, commercially pure aluminum (1050), and Al-7%Si binary alloy were investigated, using different additions of Al-10%Ti, Al-5%Ti-1%B, and Al-4%B master alloys. Thermal analysis and metallography were used to assess the variations in microstructure resulting from these additions, at solidification rates of 0.8°C/s and ~10°C/s. The results revealed that addition of Al-4%B to ultra-pure aluminum forms AlB_{12} and AlB_2 which have no grain-refining effect. Without grain refiner addition, the pure aluminum microstructure exhibits a mixture of columnar and equiaxed grains. Addition of 30ppm Ti is sufficient to promote equiaxed grains at ~10°C/s but requires addition of 1000 ppm B to obtain similar results at 0.8°C/s. Increasing the Si content to 7% reduces the initial grain size of pure aluminum from 2800 μm to ~1850 μm, and further to 450 μm with ddition of ~500ppm B. In commercial aluminum, the B reacts with traces of Ti forming Al_3Ti and TiB_2 phases which are active grain-refiners. In Al-7%Si, Ti reacts with Si forming $(Al,Si)_2Ti$ phase, which is a poor refining agent. This phenomenon is termed poisoning. No interaction between B and Si is observed in the commercial aluminum or Al-7%Si alloy when B is added.

Keywords: aluminum, grain refining, poisoning, columnar-to-equiaxed transition, solidification rate, macrostructure

1. Introduction

Master alloys of the type Al-B are largely used in production of ultra-pure aluminum to react with transition elements such as V, Cr, and Zr [1]. Boron is not considered as

effective a grain refiner when added to pure aluminum [2]. Once Si is added to Al, grain refining is activated together with a change in the α-Al dendritic structure [3]. Two types of B-compounds exist in the Al-B master alloys: AlB_2 and AlB_{12} [4]. The AlB_2 compound is stable at room temperature and contains 44.5% B [5–7]. It is inferred from the Al-B binary diagram presented in **Figure 1(a)** that there is a peritectic reaction at 975°C: L + AlB_{12} → AlB_2. A eutectic reaction (liquid → α-Al + AlB_2) takes place at 660°C, making the maximum solubility of B in Al about 20 ppm where the α-Al grains would precipitate on the AlB_2 particles. The melting points of AlB_2 and AlB_{12} are 1665 ± 50°C and 2163 ± 50°C, respectively, resulting in the formation of solid dispersoid particles in the molten liquid [8]. Fundamentally speaking, the addition of a grain refiner to the molten metal would result in the nucleation of new grains or reaction with other elements in the molten
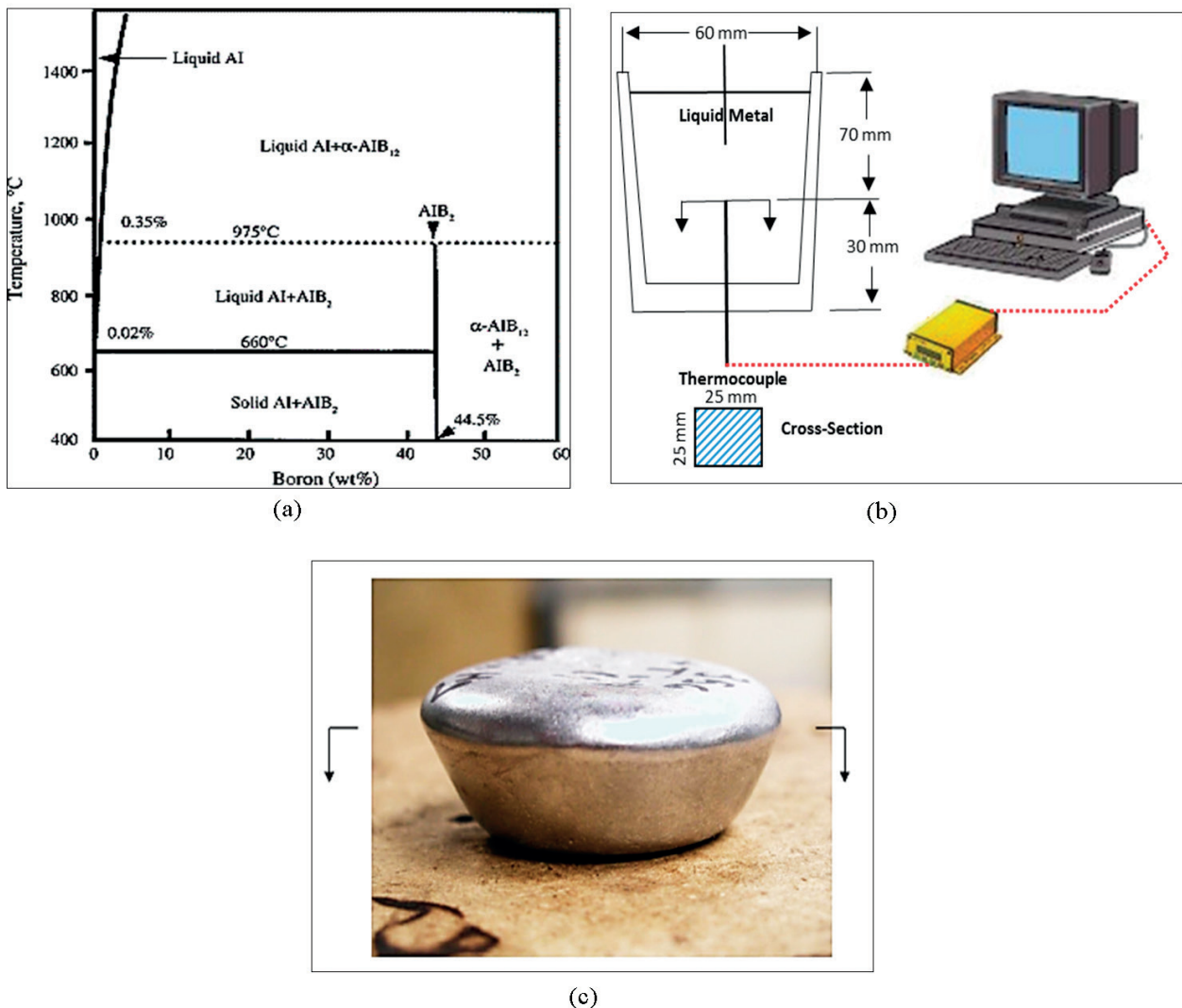

(a)

(b)

(c)

Figure 1. (a) Aluminum rich corner of Al-B phase diagram [7]. Broken arrow points to Al + AlB_2 eutectic reaction. (b) Schematic drawing showing the graphite mold used for thermal analysis. (c) Casting made in steel cups to obtain a solidification rate of 10°C/s.

metal to form nucleation sites. When Al-4%B master alloy is added to commercial aluminum containing traces of Ti, the B atoms would react with Ti forming TiB_2 phase (Ti + B → TiB_2(s)). The free energy (ΔG) associated with this reaction can be calculated as $\Delta G = -73381 + 38.996T$, where T is the liquid temperature [9]. The enthalpy energy associated with the formation of TiB_2 phase particles is fairly large – 326.41 kJ/mol—which allows for their stability in the molten metal.

In order to clarify the role of Si in activating the grain refiner, several castings were made using pure Al (99.999%), commercially pure aluminum (1050), and a binary Al-7%Si alloy. The study was conducted using thermal analysis, whereas another set of castings for grain refining was carried out using reduced pressure testing steel cups.

2. Experimental procedure

In this study, pure aluminum (99.999%), commercial pure aluminum (1050), and Al-7%Si were used. The compositions of the materials used are shown in **Table 1**. Each base alloy was melted in a resistance-heated clay graphite crucible and held at 750°C. The three grain refiners Al-10%Ti, Al-5%Ti-1%B, and Al-4%B were added to each melt in the amounts (Ti or B): 0.02–0.4% wt.%. Prior to casting, the liquid metal was held at 750°C for 10, 30, 60, 90, and 120 min after the grain refiner addition was made and then cast. During the holding time, the melt was continuously stirred using a graphite impeller to minimize sedimentation of Ti-containing particles and maintain uniformity. Samplings from the different melts prepared at 750°C were poured into a preheated (600°C) cylindrical graphite mold to achieve near-equilibrium solidification conditions (solidification rate ~0.8°C/s), as shown in **Figure 1(b)**. Another set of castings was made using steel cups of the reduced pressure testing machine in air. The steel cups were not preheated in order to obtain a high cooling rate of about 10°C/s, as shown in **Figure 1(c)**—solidification rate is about 10°C/s. Castings were also made using steel cups preheated at 450°C to represent an intermediate solidification rate. Additionally, the microstructure was evaluated at both cooling rates.

The temperature-time data was obtained using a K-type (chromel-alumel) thermocouple inserted through the bottom of the graphite mold along the centerline, its tip reaching up to about one-third the height of the mold from the bottom. The cooling curves were recorded using a data acquisition system attached to the thermocouple. Chemical analysis

Alloy	Al	Si	Cu	Mg	Fe	Mn	Zn	Ti	Sr
Al pure	99.998	0	0	0	0	0	0	0	0
1050	Bal.	0.25	0.05	0.05	0.4	0.04	0.07	<0.05	0
Al-7%Si	Bal.	6.78	0.02	00	0.03	0.04	0.04	<0.03	0

Table 1. Chemical composition (wt.%).

of all melts/castings was determined using a Spectrolab Jr CCD Spark Analyzer (average of three burns per sample).

The solidified castings were sectioned perpendicular to the centerline axis of the cylinder, at the level of the thermocouple tip, and polished for metallographic examination, using standard polishing procedures. The polished samples were examined using an optical microscope and an electron probe micro-analyzer (JEOL JXA-8900L operating at 20 kV), equipped with energy dispersive X-ray spectroscopic (EDS) and wavelength dispersive spectroscopic (WDS) facilities.

3. Results and discussion

Figure 2 shows the temperature-time curves of pure Al and Al-7%Si binary alloy after different melt treatments. **Figure 2(a)** shows that the addition of B to pure Al reduces the undercooling by approximately ~1°C, indicating the relative ineffectiveness of B as a grain refiner in the absence of Si. A 300 ppm level of B added to the Al-7%Si alloy eliminated the phenomenon of recalescence. Increasing the concentration of B to 800 ppm has minimal further effect on the alloy solidification behavior. As shown below, the transformation of AlB_{12} to a simple phase AlB_2 is the principal parameter in the disappearance of the observed undercooling shown in **Figure 2(a)**.

Figure 2(b) demonstrates the variation in aluminum grain size as a function of Sr-B interaction in the presence of 200 ppm Sr as well as holding time. In the absence of melt treatment, the average grain size was about 2900 μm. Once the two agents (B and Sr) were simultaneously added to the melt, the grain size dropped to 420 μm at 0.1%B. The observed reduction in the grain size may be interpreted in part as due to presence of traces of Ti either in the used aluminum or in the added Al-4%B master alloy as shown in **Table 2**. At higher B concentrations, the grain size tended to increase reaching 3300 μm at holding time of 120 min. This observation may be explained in terms of agglomeration of the nucleation sites [10]. As shown in **Table 1**, a eutectic reaction takes place at about 660°C; Liquid → $AlB_2 + \alpha$ (solid). In Si-containing aluminum alloys, i.e., 356 alloy, the melting point is less than the eutectic temperature, which facilitates the formation of AlB_2, an active nucleation agent. The melting temperature of pure Al is about 660.5°C, and hence the reported sluggishness of B as a grain refiner in pure Al [11]. **Figure 2(c)** displays the variation in the grain size of Al-7%Si alloy as a function of holding time when the alloy was grain refined using Al-4%B master alloy in the presence of 200 ppm Sr. Due to high Si content, the initial grain size dropped to approximately 1850 μm. With the addition of approximately 500 ppm B, the grain size was reduced to about 450 μm (~75%). Holding time up to 120 min seems to have a marginal effect on further decrease in the alloy grain size. These findings are in good agreement with the abovementioned discussion.

Figure 3 reveals the possibility of the coexistence of the two B-based compounds in pure aluminum. The composition of these two phases was confirmed using the WDS technique as shown in **Table 3**. **Figure 4** shows the distribution of B- (black), and Si-phases (light gray)
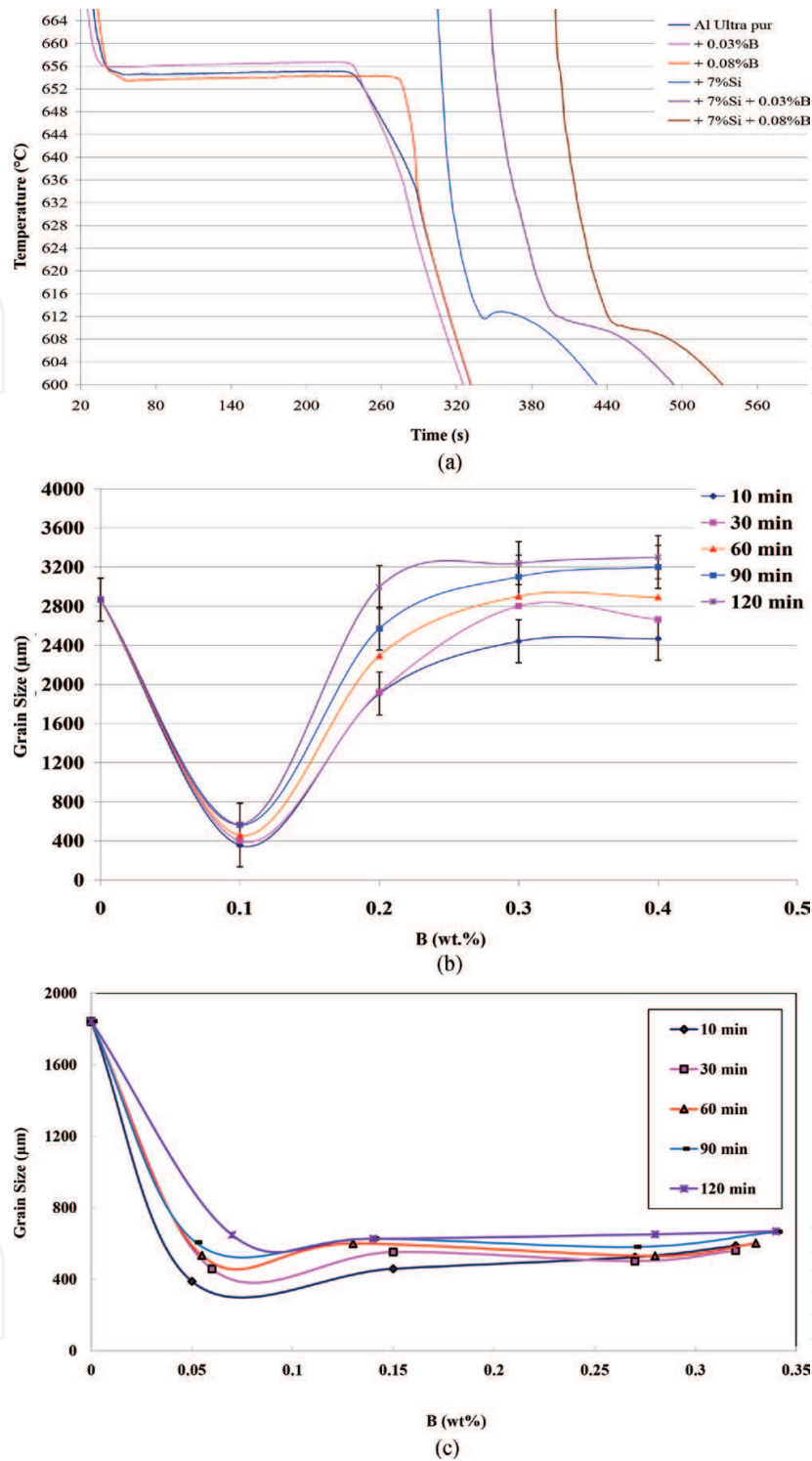
Figure 2. (a) Temperature-time solidification curves obtained from pure Al and Al-7%Si alloy following different melt treatments. (b) Effect of Sr-B interaction on the pure aluminum grain size as a function of holding time. (c) Effect of Sr-B interaction on the grain size of Al-7%Si alloy as a function of holding time.

in Al-7%Si alloy. As can be seen, these elements tend to precipitate away from each other (marked zones A and B in **Figure 4**). This observation is confirmed by the X-ray elemental distribution for each zone shown in **Figure 5**, indicating that there is no affinity for reaction

Pure Al, series Al-4%B

| Holding time (min)	Trial #	wt.% B addition	wt.% Si	B (ppm)	% Ti	Added Sr (ppm)	Actual Sr (ppm)
10	1	0.1	0.062	78	0.0403	200	145
	2	0.2	0.062	114	0.0104	200	195
	3	0.3	0.063	206	0.005	200	155
	4	0.4	0.068	189	0.0031	200	125
30	1	0.1	0.062	132	0.0342	200	101
	2	0.2	0.066	203	0.005	200	143
	3	0.3	0.064	147	<0.0013	200	145
	4	0.4	0.077	225	0.0019	200	95
60	1	0.1	0.054	84	0.0401	200	64
	2	0.2	0.063	93	<0.0013	200	106
	3	0.3	0.063	>360	0.0027	200	110
	4	0.4	0.061	104	0.0041	200	61
	5						
90	1	0.1	0.06	48	0.0249	200	51
	2	0.2	0.064	148	<0.0013	200	74
	3	0.3	0.07	165	<0.0013	200	80
	4	0.4	0.057	90	<0.0013	200	49
	5						
120	1	0.1	0.065	153	0.0367	200	58
	2	0.2	0.066	49	<0.0013	200	50
	3	0.3	0.0742	>360	0.0027	200	53
	4	0.4	0.059	121	0.0014	200	66

Table 2. Chemical analysis of melt treated pure aluminum samples.

between these two elements In contrast, when Ti is added with B to the 1050 commercial aluminum, a clear interaction between Ti and B takes place leading to the formation of TiB_2, as demonstrated in **Figure 6**. Thus, B has no grain-refining capacity when added as a single element to ultra-pure aluminum, whereas when the metal contains traces of Ti, adding B leads to the possible formation of different nucleation sites that coexist, such as AlB_{12}, AlB_2, and TiB_2 in Al-Si alloys.

It is well established that increasing solidification rate significantly enhances grain-refining effects [12–14]. In order to illustrate this, samples were poured into steel cups of the reduced pressure testing machine (about 200 g) in air corresponding to a solidification rate of about
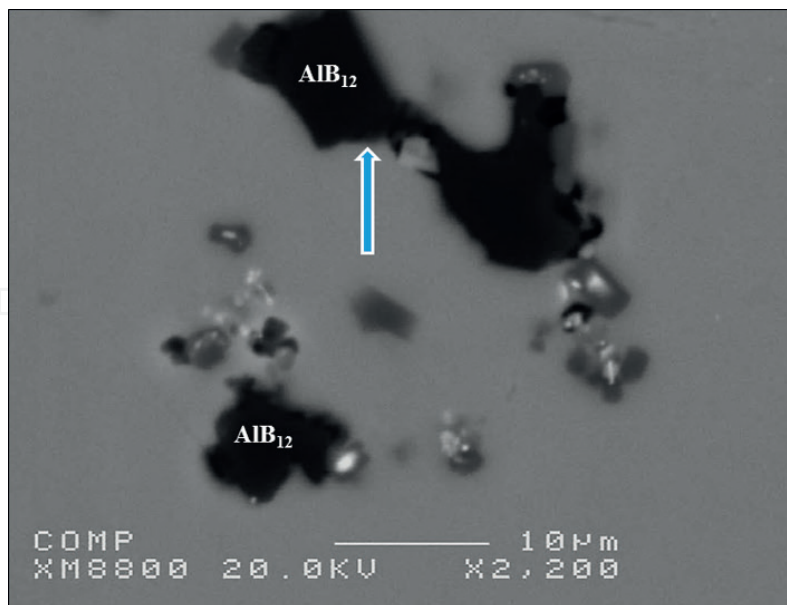
(a)
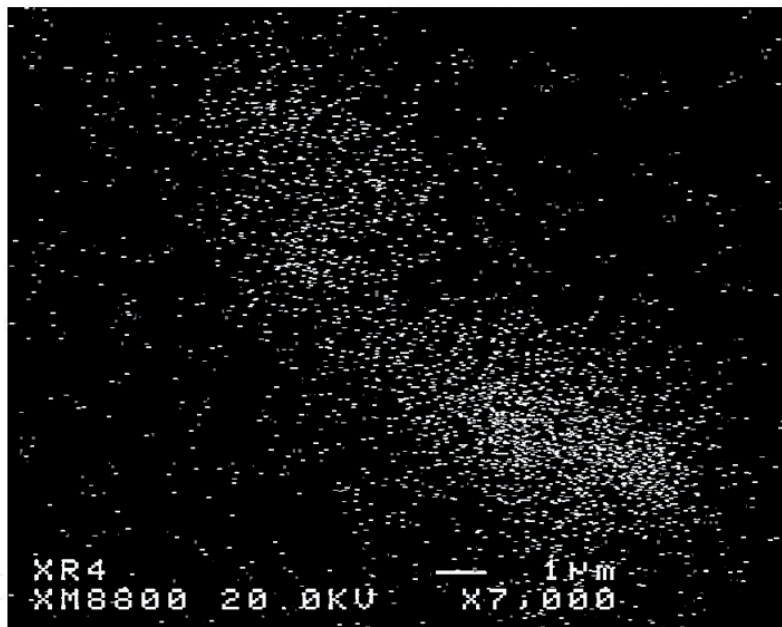
(b)

Figure 3. (a) Presence of AlB_{12} in ultra-pure aluminum (possible decomposition of AlB_{12} to AlB_2), (b) X-ray image of B distribution in AlB_{12} phase particles in (a)-arrowed.

$10°C/s$ [13, 14]. In the absence of a grain refiner, the macrostructure of pure aluminum is composed of three zones: (i) columnar near the bottom of the crucible due to the development of positive thermal gradient in the liquid metal leading to formation of grains with preferred orientation [14], (ii) fine equiaxed grained zone, and (iii) coarse grained zone where the grains are randomly oriented caused by fragmentation of the columnar grains driven by convection in the liquid metal, as illustrated in **Figure 7** for samples solidified at $0.8°C/s$. The equiaxed

Al	B	Phase
34.15	63.19	AlB$_2$
35.40	64.47	
31.47	66.64	
33.62	65.51	
7.32	91.56	AlB$_{12}$
8.52	90.78	

Table 3. WDS analysis (at.%) of AlB$_2$ and AlB$_{12}$ phases observed in **Figure 3(a)**.

crystals have a larger size than the chilled ones, and they are the result of volumetric solidification, which proceeds when the initially high thermal gradient is reduced as solidification progresses [15]. The refinement of the primary structure is a result of the creation of phases that act as substrates of heterogeneous nucleation for the primary aluminum phase. Therefore, active centers of aluminum heterogeneous nucleation are particles that have a high melting point and close crystallographic match with aluminum, e.g., TiC, TiN, TiB, TiB$_2$, AlB$_2$, Al$_3$Ti, and Zn$_3$Ti [16–20].

When an Al-5%Ti-1%B master alloy is added to pure aluminum, it decomposes into Al$_3$Ti and TiB$_2$ phase particles. Since the dissolution of Al$_3$Ti is rather fast in Al-Si alloys, it forms Ti(Sl$_{1-x}$,Si$_x$)$_3$ where $x < 0.15$ [21]. The latter tends to cover the TiB$_2$ particle surface acting as a heterogeneous nucleation substrate for the α-Al through the peritectic reaction. The addition of 600 ppm Ti in the form of Al-10%Ti to pure aluminum (**Figure 7(b)**) resulted in the complete elimination of the columnar grains with marked reduction in the grain size of the two equiaxed zones observed in **Figure 7(a)**. Increasing the Ti concentration to 1000 ppm led
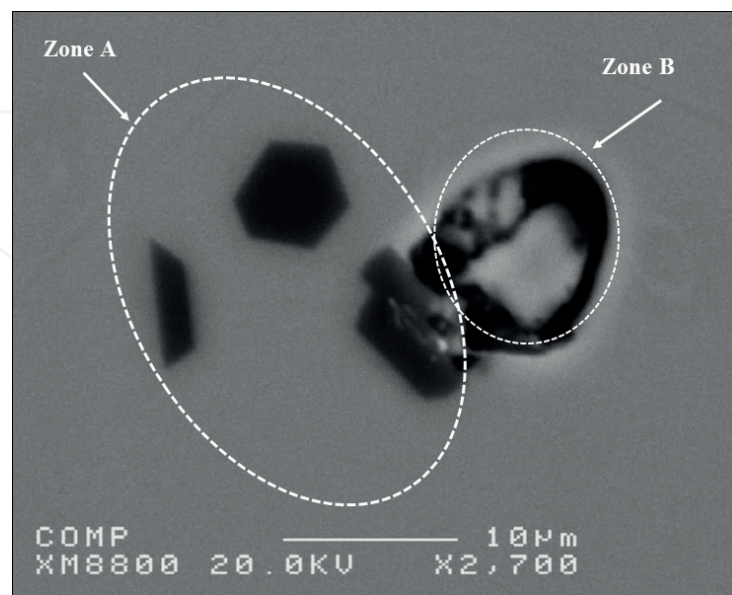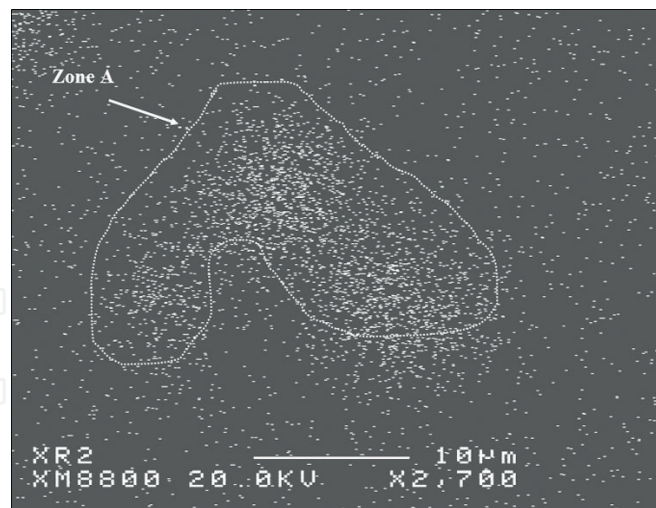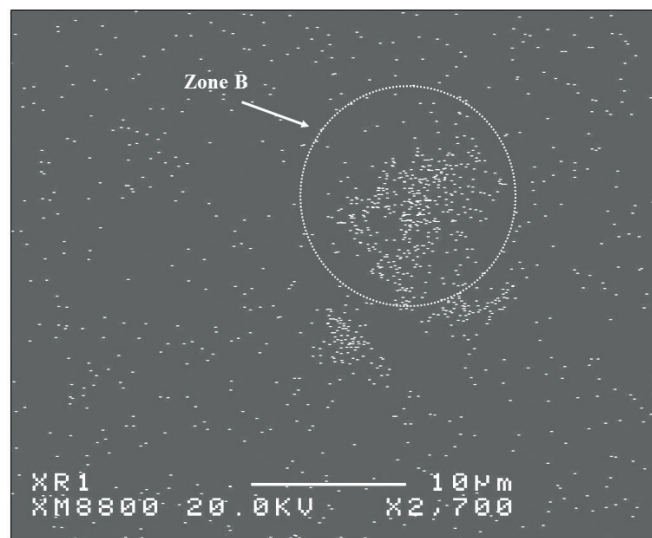

Figure 4. Presence of B and Si in Al-7%Si treated with 800 ppm B. Note the geometric shape of the particles in zone A.

Figure 5. Selected X-ray for B and Si distribution of (a) B (b) Si in **Figure 4**—Al-7%Si alloy treated with 800 ppm B.

to formation of one zone characterized by its ultra-fine grain size (**Figure 7(c)**). Similar observations were made when the liquid aluminum was treated with Al-5%Ti-1%B master alloy (**Figure 7(d** and **e)**).

As previously mentioned, B has no grain-refining effect on ultra-pure aluminum. However, if its addition is associated with a relatively high cooling rate, i.e., 10°C/s as shown in **Figure 8**, it could result in some refining depending on B concentration as shown in **Figure 8(d)**, where at least 1000 ppm B is used to obtain more or less same level of grain size produced by the addition of 30 ppm TiB$_2$ (**Figure 7(e)**). These experiments always produced a grain size gradient from the bottom of the crucible to the top surface. This is usually attributed to the fact that the crucible surface acts as a nucleation substrate for heterogeneous nucleation of α-Al. In addition, once solidification initiates on the relatively cold bottom of the crucible, sensible and latent heat are released to the crucible, reducing the temperature gradient and effectively slowing
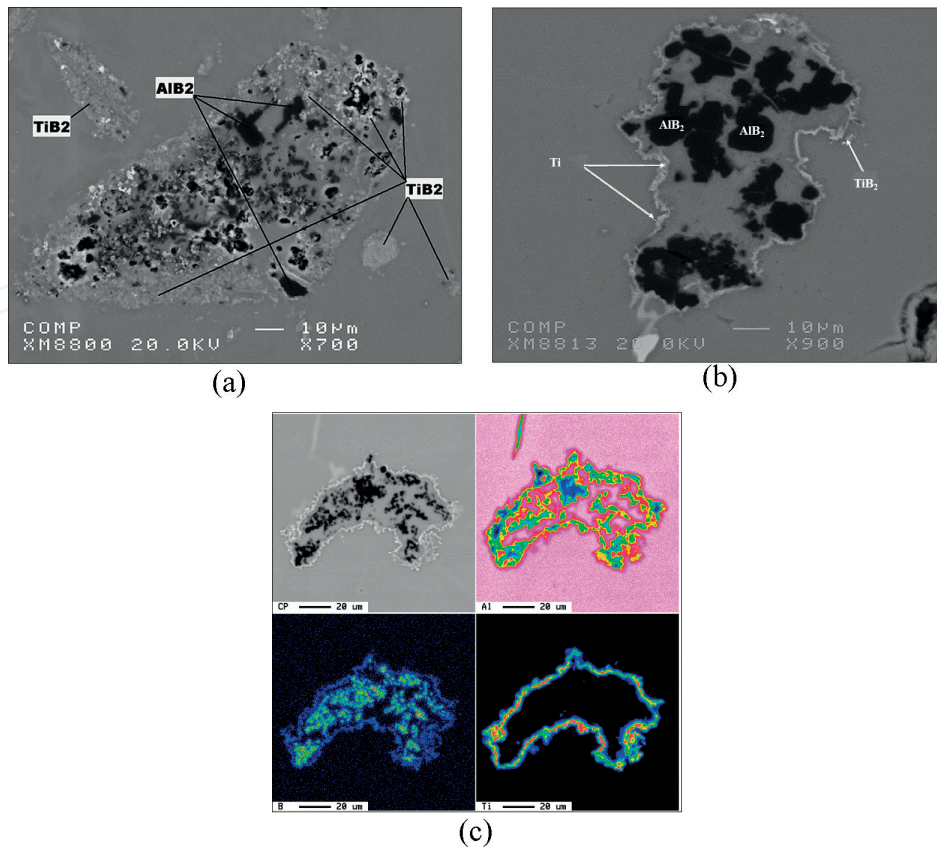
(a)   (b)

(c)

Figure 6. (a) Decomposition of Al-5%Ti-1%B master alloy, (b) backscattered electron image and (c) element distribution of Ti-B interaction in 1050 aluminum treated with 240 ppm B. Note the attraction of Ti ring toward the cluster of B-rich particles.
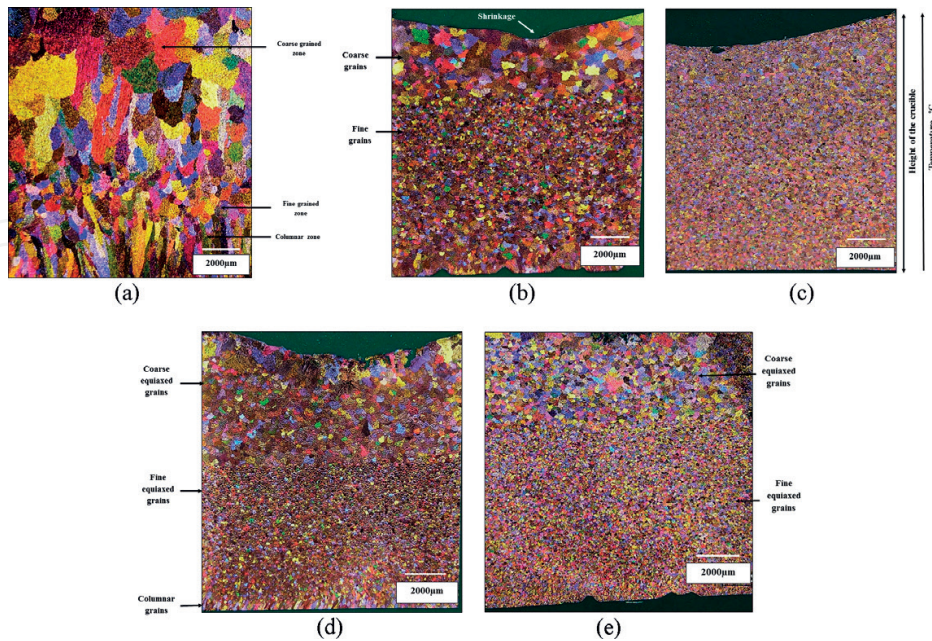

(a)   (b)   (c)

(d)   (e)

Figure 7. Macrostructures of ultra-pure aluminum treated by two types of grain refiners: (a) Al pure (no treatment), (b) Al pure + Al_3Ti (600 ppm), (c) Al pure + Al_3Ti (1000 ppm), (d) Al pure + TiB_2 (15 ppm), (e) Al pure + TiB_2 (30 ppm). All micrographs have same magnification-solidification time was ~200 s. Note the heterogeneity in grain size on going from bottom to top.
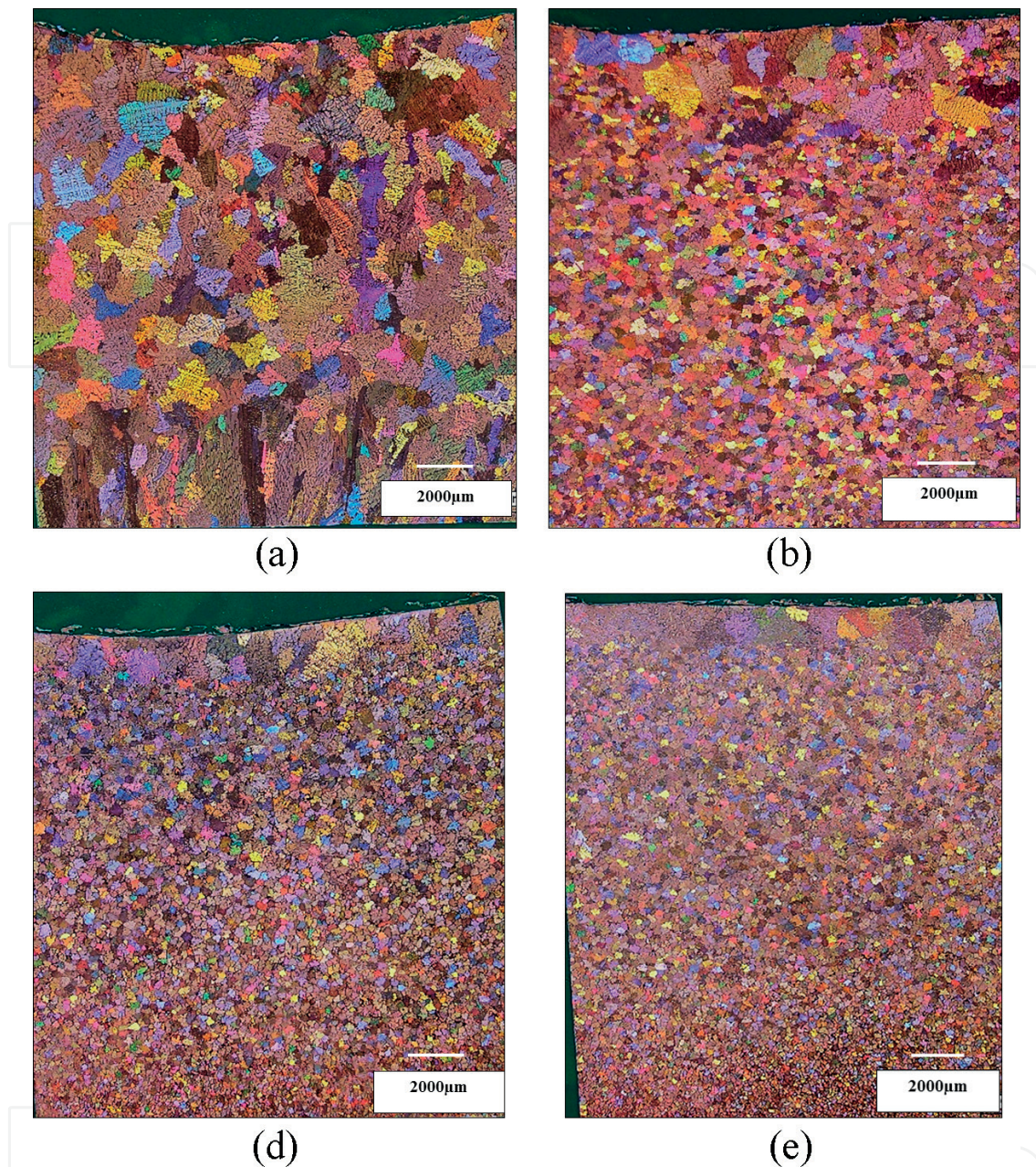
Figure 8. Macrostructures of ultra-pure aluminum treated with progressive doses of B: (a) 30 ppm B, (b) 60 ppm B, (c) 120 ppm B, (d) 1000 ppm B. All micrographs have the same magnification. Note the progressive transition from columnar-to-equiaxed (CTE) with the increase in B concentration.

the solidification rate. According to Chalmers [15], predendritic solid nuclei that formed on the mold surface during filling of the mold are driven away by circulation of the liquid metal. Depending on the degree of undercooling, some of these nuclei would survive in the liquid until the undercooling is extracted, resulting in equiaxed grains.

Considering the Al-7%Si alloy, its structure was not affected by the phenomenon mentioned above in the case of ultra-pure aluminum. **Figure 9** shows the macrostructure of the alloy with different melt treatments consisting of fine equiaxed grains caused by the addition of a suitable dose of grain refiner associated with application of high solidification rate—note
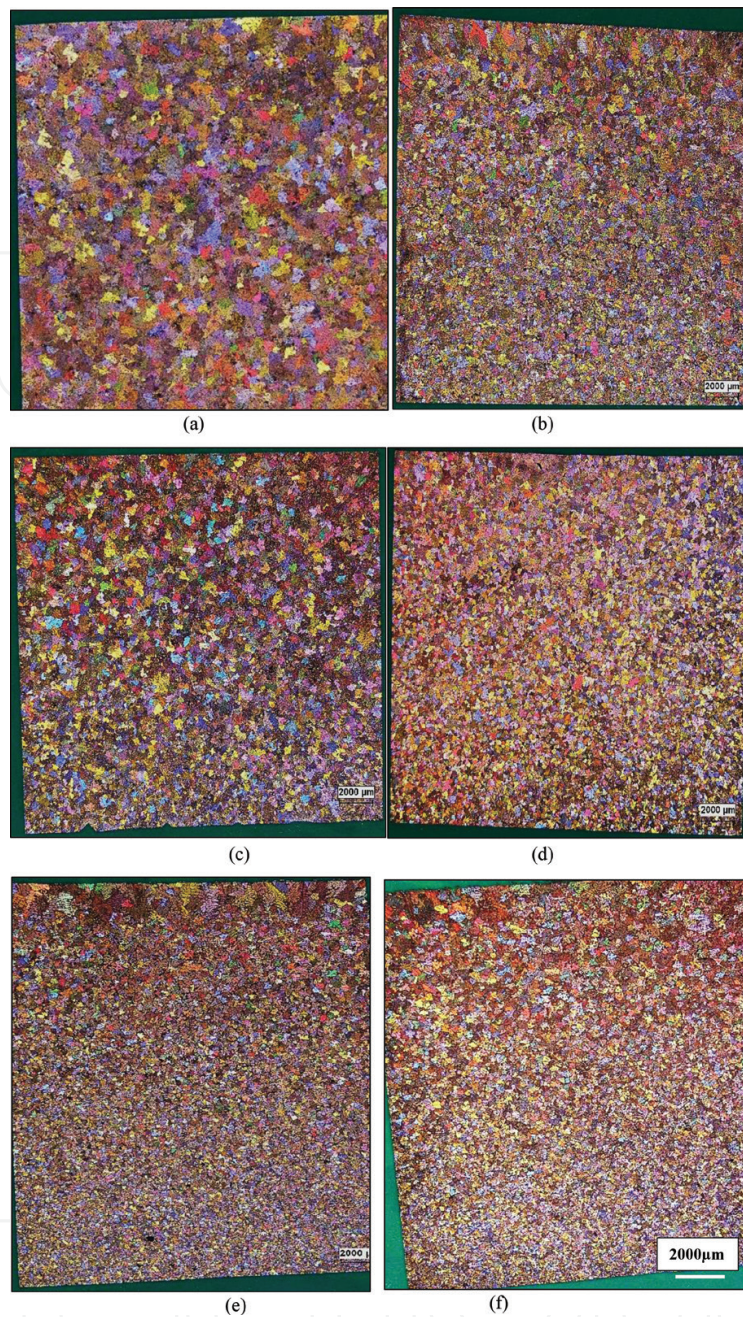
Figure 9. Variation in the grain size of Al-7%Si alloy: (a) base alloy—no addition, (b) alloy treated with Al-10%Ti (300 ppm Ti), (c) alloy treated with Al-5%Ti-1%B (150 ppm of B), (d) alloy treated with Al-5%Ti-1%B (300 ppm of B), (e) alloy treated with Al-4%B (600 ppm B), (f) alloy treated with 1000 ppm B. All micrographs have the same micron bars.

the absence of columnar grains. The transition from columnar to equiaxed grains depends on several factors: (i) mold geometry, (ii) the amount of extracted heat, (iii) composition of used alloy, (iv) density of the used grain refiner, (v) fluidity of the liquid metal, (vi) interaction between grain refiner and alloy composition and (vii) sedimentation of the added grain refiner [22]. A high solidification rate, large amount of grain refiners as well as low temperature gradient would enhance fine equiaxed grains [23]. Al-7wt.% Si alloys with and without grain refiners solidified in diffusive conditions showed columnar growth in case of nonrefined alloy, and the existence of a columnar-to-equiaxed transition (CTE) in refined alloy. A sharp CTE is

observed when increasing the solidification rate and a progressive CTE when lowering the temperature gradient [24].

4. Concluding remarks

The results obtained show that when Al-4%B is added to ultra-pure aluminum, it decomposes into AlB_{12} and AlB_2 phases that have no grain-refining effect in pure aluminum. When no grain refiner is added to pure aluminum, the microstructure is a mixture of columnar and equiaxed grains. The addition of 30 ppm Ti to pure aluminum is sufficient to promote equiaxed grains when the metal is solidified at high rate (~10°C/s). A similar effect can be achieved with the addition of excessive amounts of B, in the order of 1000 ppm. Increasing the Si content to 7% enhances the reduction in initial grain size of pure aluminum from 2800 to 1850 μm in Al-7%Si alloy. In the case of Al-7%Si, only 500 ppm B is sufficient to reduce the initial grain size by about 75%. Due to a reduced temperature gradient as the solidification front travels from the bottom of the crucible to the top, the grain size varies accordingly.

In commercial aluminum, the addition of B would react with traces of Ti leading to the formation of Al_3Ti and TiB_2 phases that are effective grain-refining agents. In the case of Al-7%Si, Ti reacts with Si forming $(Al, Si)_2Ti$ phase which is a poor refining agent. This phenomenon is termed *poisoning*. No interaction was observed to take place between B and Si. In general, the grain size varied along the height of the crucible due to change in the liquid temperature.

Acknowledgements

Conflict of interest

There is no conflict of interest between the authors.

Author details

Hicham Tahiri[1], Serageldin S. Mohamed[1], Herbert W. Doty[2], Salvador Valtierra[3] and Fawzy H. Samuel[1]*

*Address all correspondence to: fhsamuel@uqac.ca

1 Département des Sciences Appliquées, Université du Québec à Chicoutimi, Québec, Canada

2 General Motors Materials Engineering, Pontiac, MI, USA

3 Nemak, S.A., Garza Garcia, N.L., Mexico

References

[1]   Stiller W, Ingenlath T. Industrial boron treatment of aluminium conductor alloys and its influence on grain refinement and electrical conductivity. Aluminium. Vol. 60; 1984. pp. E577-E580

[2]   Cooper PS, Kearns MA. Removal of transition metal impurities in aluminium melts by boron additives. Trans Tech Publications Ltd. Aluminium Alloys: Their Physical and Mechanical Properties. Zurich, Switzerland. Vol. 217; 1996. pp. 141-146

[3]   Wang GQ, Liu SH, Li CM, Gao Q. Reaction of boron to transition metal impurities and its effect on conductivity of aluminum. Transactions of Nonferrous Metals Society of China. 2002;**12**:1112-1116

[4]   Alamidari HD, Dube D, Tessier P. Behavior of boron in molten aluminum and its grain refinement mechanism. Metallurgical & Materials Transactions A. 2013;**44A**:388-394

[5]   Mondolfo LF. Aluminum Alloy Structure and Properties. London: Butterworth; 1976

[6]   Sigworth GK. The grain refining of aluminum and phase relationships in the aluminum-titanium-boron system. Metallurgical Transactions A: Physical Metallurgy and Materials Science. The Metallurgical Society of AIME and American Society for Metals, USA. Vol. 15A; 1984. pp. 277-282

[7]   Rogl P, Schuster JC. Phase Diagrams of Ternary Boron Nitride and Silicon Nitride System. ASM International; Materials Park, OH, USA. 1992

[8]   Giardini AA, Kohn JA, Toman L, Eckart DW. Boron—Synthesis, Structure and Properties. New York: Plenum Press; 1960. pp. 140-158

[9]   Li H, Sritharan T, Lam YM, Leng NY. Effects of processing parameters on the performance of Al grain refinement master alloys Al-Ti and Al-B in small ingots. Journal of Materials Processing Technology. 1997;**66**:253-257

[10] Khalifa W. Rôle des inclusions dans la germination de la phase α-Aluminium et des intermétalliques contenant du fer dans le coin riche en aluminium du système ternaire Al-Si-Fe. thèse présentée à l'Université du Québec à Chicoutimi UQAC, novembre 2003. p. 340

[11] Lu HT, Wang LC, Kung SK. Grain refining in A356 alloys. Journal of Chinese Foundryman's Association. 1981;**29**:10-18

[12] Samuel AM, Samuel FH. Use of the reduced pressure test in the measurement of the hydrogen content in the foundry of composites. In: Proceedings International Symposium on "Advances in the Production of Light Metals and Metal Matrix Composites", 31st Annual Conference of Metallurgists of CIM, Edmonton, Alberta, Canada, August 23-27, 1992; Edmonton, AL, Canada. pp. 701-715

[13] Samuel AM, Samuel FH. The reduced pressure test as a measuring. Metallurgical Transactions A. 1993;**24**:1857-1868

[14] Kurz W, Bezençon C, Gäumann M. Columnar to equiaxed transition in solidification processing. Science and Technology of Advanced Materials. 2001;**2**:185-191

[15] Chalmers B. The structure of ingots. Journal of the Australian Institute of Metals. 1963;**8**:255-263

[16] Guzowski M, Sigworth G, Sentner D. The role of boron in the grain refinement of aluminum with titanium. Metallurgical Transactions A. 1987;**18**:603-619

[17] Wróbel T. Review of inoculation methods of pure aluminum primary structure. Archives of Materials Science and Engineering. 2011;**50**:110-119

[18] Greer. Structure and properties of grain-refined Al-20 wt.% Zn sand cast alloy. Metallurgy and Materials. 2009;**54**:329-334

[19] Haberl K, Krajewski WK, Schumacher P. Microstructural features of the grain-refined sand cast AlZn20 alloy. Metallurgy and Materials. 2010;**55**:837-841

[20] Wróbel T, Szajnar J. Influence of supply voltage frequency of induction coil on inoculation efficiency of pure aluminum structure. Foundry Engineering. 2010;**10**:203-208

[21] Hodaj F, Durand F. Equiaxed grains in multicomponent alloys: Effect of growth rate. Acta Materialia. 1997;**45**:2121-2127

[22] Sturz L, Zimmerman G. Investigations on columnar to equiaxed transition in binary Al alloys with and without grain refiners. Materials Science Forum. 2006;**508**:419-424

[23] Sturz L, Drevermann A, Pickmann C, Zimmermann G. Influence of grain refinement on the columnar-to-equiaxed transition in binary Al alloys. Materials Science and Engineering A. 2005;**413-414**:379-383

[24] Zimmermann G, Sturz L, Billia B, Mangelinck-Noël N, Liu DR, Nguyen Thi H, Bergeon N, Gandin Ch-A, Browne DJ, Beckermann Ch, Tourret D, Karma A. Columnar-to-equiaxed transition in solidification processing of AlSi7 alloys in microgravity-The CETSOL project. Materials Science Forum. 2014;**790**:12-21